Study on effect of carburizing on microstructure and high temperature oxidation properties of hot dip aluminum coating on titanium alloy

Wenying Yang and Faguo Li *

Posted Date: 23 June 2023

doi: 10.20944/preprints202306.1678.v1

Keywords: titanium alloy; Ti-Al alloy phase layer/Ti-Al carburizing composite coating; hot dip aluminization; carburizing; thermal exposure test

Article

Study on effect of carburizing on microstructure and high temperature oxidation properties of hot dip aluminum coating on titanium alloy

Wenying Yang, Faguo Li*

School of Materials Science and Engineering, Xiangtan University, Xiangtan, Hunan, China, 411105
yangwenying0510@163.com (W.Y.)
* Correspondence author: lifaguo@xtu.edu.cn (F.L.)

Abstract: Ti-Al alloy phase layer/Ti-Al carburizing composite coating was prepared on the surface of titanium alloy by the stepwise coating method of hot dip aluminization and then carburizing. The weight gain results of the composite coating showed that the titanium alloy coated with the composite coating had long-term stability (≥16 days) at 800°C. The microstructure, phase structure and composition of the composite coating were characterized by X-ray diffraction (XRD), scanning electron microscopy (SEM) and energy dispersive spectroscopy (EDS).The composite coating is composed of an alloy phase layer and a carburized layer. The natural transition of four phases (Ti_3Al/TiAl/$TiAl_2$/$TiAl_3$) in the alloy phase layer, significantly improves the interfacial bonding between the coating and the substrate, and slows down the propagation of microcracks through the coating.Al_2O_3, TiC and C in the carburizing layer improve the surface hardness of the coating, and $TiAl_2$ and Al_2O_3 also have excellent oxidation resistance at high temperature.

Keywords: titanium alloy; Ti-Al alloy phase layer/Ti-Al carburizing composite coating; hot dip aluminization; carburizing; thermal exposure test

1. Introduction

Aero-engine is known as the "heart" of aircraft, and the progress of its design, material and manufacturing technology plays a key role in the development of aviation industry. Advanced aero-engines are developing towards high turbine front temperature, high thrust-to-weight ratio, long life and low fuel consumption. In addition to advanced design technology, the improvement of engine performance strongly depends on the development of advanced materials and manufacturing technology.

Titanium alloy is widely used in the aerospace field because of its advantages such as low density, high specific strength, corrosion resistance and stable performance at low temperature[1-4], and is known as "space metal". However, titanium alloy's poor high-temperature oxidation resistance[5], low surface hardness, high friction coefficient and poor wear resistance seriously restrict its service life and application field [6]. In order to effectively improve the properties of titanium alloy, the most widely used method is to prepare aluminum coating with excellent oxidation resistance on the surface of titanium alloy.

The formation of Ti-Al diffusion coating on titanium alloy is a common method to improve its high-temperature oxidation resistance [7, 8]. The Ti-Al diffused coating can

Preprints (www.preprints.org) | NOT PEER-REVIEWED | Posted: 23 June 2023 doi:10.20944/preprints202306.1678.v1

be prepared by different processes such as thermal spraying[9], aluminizing[10], laser surface alloying[11], sol-gel method [12] and hot dip aluminizing [7]. Hot dip aluminizing is a mature and extensible process [13, 14]. Hot dip aluminizing process includes surface pretreatment of the sample and holding in molten aluminum pool for a certain time. This method was first applied to stainless steel, carbon steel and alloy steel, often used to improve the corrosion resistance, wear resistance and high temperature oxidation resistance [15-17]. $TiAl_3$ phase +L-(Ti,Al) and L-(Ti,Al) layers are formed on the surface of titanium alloy after hot dip aluminization. Due to the brittleness of $TiAl_3$ phase and the mismatch of thermal expansion coefficient between $TiAl_3$ phase and titanium alloy substrate [18], the mechanical properties of substrate are reduced and cracks are easy to propagate. Therefore, proper heat treatment is required after hot dip aluminizing to make elements diffuse between coating and substrate, so as to produce metallurgical bonding between coating and substrate[19]. The L-(Ti,Al) layer on the surface is mainly aluminum, and its wear resistance and hardness are insufficient. Surface modification of L-(Ti,Al) layer to improve its wear resistance, surface hardness and reduce friction coefficient is an urgent requirement to improve its application in various fields.

In the process of carburizing, carbon atoms penetrate into the surface of titanium alloy through concentration gradient at high temperature to form the corresponding carbide (TiC) gradient coating. The advantage of carburizing on titanium alloy is to effectively improve the surface hardness and wear resistance of the material without changing the substrate properties and macroscopic size. The gradient structure coating is grown by in-situ extension, which significantly improves the interface bonding between the coating and the substrate and eliminates the mismatch of thermal expansion coefficient and weak adhesion[20]. However, the thickness of the coating prepared by this method is limited, generally only a few microns to tens of microns.

We combine the hot dip aluminizing process with carburizing process to give full play to the advantages of both and achieve the optimization effect of "1 + 1 > 2". When the titanium alloy after hot dip aluminization is carburizing, the surface L-(Ti,Al) layer reacts with active carbon atoms to form Ti-Al carburizing layer with good wear resistance and high hardness. The aluminum element in $TiAl_3$ phase continues to diffuse to the substrate, and Al reacts with Ti to form more Ti-Al alloy phase layers. Finally, Ti-Al alloy phase layer/Ti-Al carburizing layer composite coating is formed. The composite coating has the advantages of close bonding with the substrate and excellent oxidation resistance at high temperature.

In this paper, the hot dip aluminization and carburizing of Ti65 samples were studied, and the high temperature oxidation resistance of the obtained samples was analyzed. The microstructure, morphology and growth kinetics of the coatings before and after thermal exposure test were studied, and the internal reasons for the good high temperature oxidation resistance of the titanium alloy after hot dip aluminization and carburizing were discussed.

2. Materials and Methods

2.1. Experimental material

Preprints (www.preprints.org) | NOT PEER-REVIEWED | Posted: 23 June 2023 doi:10.20944/preprints202306.1678.v1

High purity aluminum ingot (99.999%), carburizing agent (charcoal, $NaCO_3$, $BaCO_3$, $CaCO_3$), Ti65 alloy, its components were: Ti - 5.9 - Al - 4.0 - Sn - 3.5 - Zr - 0.3 Mo - 0.3 Nb - Ta Si - 0.4-2.0 1.0 W - 0.05 C (wt. %), linear cutting into 15 mm (length) x 10 mm (width) x 3 mm (thickness) of the sample; All samples were polished with 400#, 600#, 800# sandpaper to ensure a smooth surface.

2.2. Hot dip aluminizing

After several Ti65 samples were cleaned with acetone for 5min, washed with water and cleaned with alcohol for 15min, they were immersed in pure aluminum liquid protected by argon at 760°C for 5min, 10min, 15min and 20min respectively. Then, the Ti65 samples were slowly extracted and the excess aluminum liquid on their surface was removed.

2.3. Carburizing

The hot dip aluminized Ti65 samples were placed in a corundum crucible equipped with solid carburizing agent and sealed with a mixture of calcined kaolin and sodium silicate. Then the sealed crucible was dried in an oven for 2h and then put into a box-type resistance furnace (Xiangtan Samsung Instrument Co., LTD, Xiangtan, China) for carburizing. The samples were kept at 1050°C for 2h, 4h, 6h and 8h respectively, and then removed after cooling to room temperature in the furnace.

2.4. Representation

The phase of the coating was analyzed by X-ray diffraction (XRD). Ultima IV diffractometer with Cu Ka radiation (λ=0.15406nm). The working voltage of the X-ray tube is 40 kV and the working current is 40 mA, and the XRD spectra obtained are in the range of 10°-90°. The Angle step is 0.02° and the scanning speed is $10°min^{-1}$.

Using scanning electron microscopy (SEM) (ZEISS EVO MA10, ZEISS, Jena, Germany) and Energy Dispersion Spectroscopy (EDS) (OXFORD X-MAXN, ZEISS, Jena, Germany) system for the analysis of the coating morphology and element distribution.

2.5. Thermal exposure test

For comparison, uncoated Ti65 samples, hot dip aluminizing (760°C×10min) Ti65 samples, hot dip aluminizing (760°C×10min) and carburizing (1050°C×4h) Ti65 samples (represented by group A, B and C below) were placed in static air at 800°C at the same time for thermal exposure test. The duration varied from 2 to 16 days, with 2 day intervals, and 3 samples were consumed for each thermal exposure time. Before and after the thermal exposure test, an electronic balance was used to weigh and record (the measurement accuracy of weight is $\pm 10^{-4}$ g), so as to calculate the weight gain per unit area of the sample at different times, and obtain the high temperature oxidation weight gain curve. The microstructure, phase composition and element distribution of the coating were studied by X-ray diffractometry (XRD), scanning electron microscopy (SEM) and energy dispersive spectroscopy (EDS).

Preprints (www.preprints.org) | NOT PEER-REVIEWED | Posted: 23 June 2023 doi:10.20944/preprints202306.1678.v1

3. Results

3.1. Characterization of coating microstructure

3.1.1. Microstructure of composite coating

Figure 1 shows the cross section microstructure of Ti-Al alloy phase layer/Ti-Al carburizing composite coating obtained by hot dip aluminizing (760°C×10min) and carburizing (1050°C×4h). It can be observed that the coating has obvious stratification, consisting of two regions, one is the alloying phase layer region, and the other is the carburizing layer region.

EDS data of different regions are shown in Table 1. EDS data of alloy phase layer region indicate that four Ti-Al diffusion layers are formed between coating and substrate. In addition, some voids were observed in the coating. The atomic ratios of Ti and Al at positions 1, 2, 3 and 4 are 3:1, 1:1, 1:2 and 1:3, respectively. Combined with the XRD pattern shown in Figure 2, the four phases are Ti_3Al, TiAl, $TiAl_2$ and $TiAl_3$, respectively.

One of the causes of the holes in the coating is the Kirkendall effect. Al [21] in $TiAl_3$ diffuses with Ti in the substrate, and the diffusion rate of Al is much higher than that of Ti [22], so the net diffusion is manifested as Al in $TiAl_3$ diffuses into Ti65 substrate, resulting in the vacancy at the edge of $TiAl_3$ phase [23, 24], and the accumulation of vacancy leads to the formation of Kirkendall void [25]. Another reason is the brittleness and large thermal expansion coefficient of $TiAl_3$ phase, which leads to the formation of cavity in the cooling process [26].

Figure 3 shows that C and O elements are mainly distributed in the carburized layer. EDS results and XRD patterns of the carburized layer indicate that the region is composed of Al_2O_3, $TiAl_2$, TiC and free C. In Figure 1(a), the white part at the top of the coating is $BaAl_2O_4$, $BaTiO_3$ and free C. The $BaAl_2O_4$ phase and $BaTiO_3$ phase are generated by the reaction of the energizer $BaCO_3$ with Al and Ti atoms in the process of carburizing, while the free C is formed by the carbon in the carburizing agent remaining in the sag on the surface of the sample.

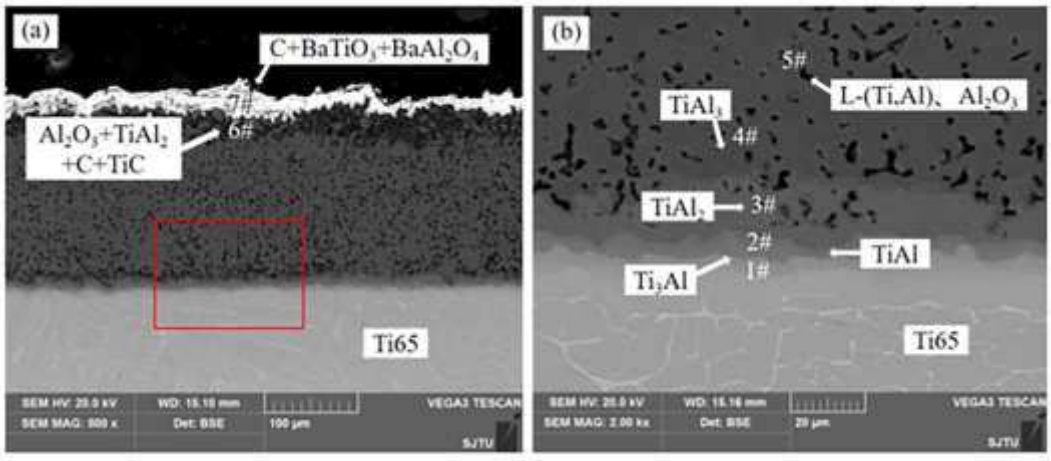

Figure 1. (a) Cross section microstructure of composite coating obtained by hot dip aluminizing (760°C×10min) and carburizing (1050°C×4h); **(b)** Enlarge part of the red wire frame in (a)

Table 1. EDS data (at.%) and phase composition in different regions

Preprints (www.preprints.org) | NOT PEER-REVIEWED | Posted: 23 June 2023 doi:10.20944/preprints202306.1678.v1

Point	Ti	Al	C	O	Ba	Compounds
1#	71.61	28.39	0	0	0	Ti_3Al
2#	48.38	51.62	0	0	0	TiAl
3#	39.08	60.92	0	0	0	$TiAl_2$
4#	27.37	72.63	0	0	0	$TiAl_3$
5#	24.94	61.62	0	13.43	0	L-(Ti,Al)、Al_2O_3
6#	4.85	25.92	14.11	55.12	0	Al_2O_3、$TiAl_2$、C、TiC
7#	2.78	10.62	21.88	53.30	11.01	$BaAl_2O_4$、$BaTiO_3$、C

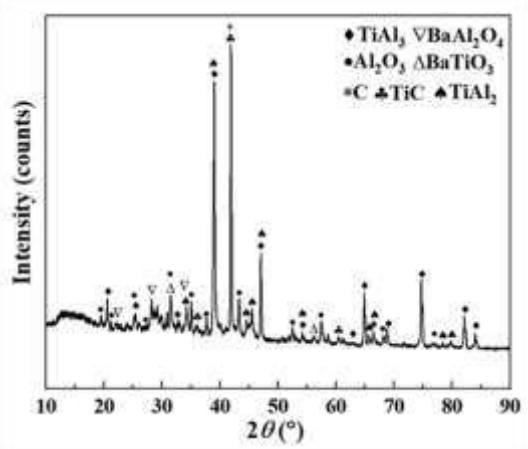

Figure 2. XRD pattern of the composite coating obtained by hot dip aluminizing (760°C×10min) and carburizing (1050°C×4h)

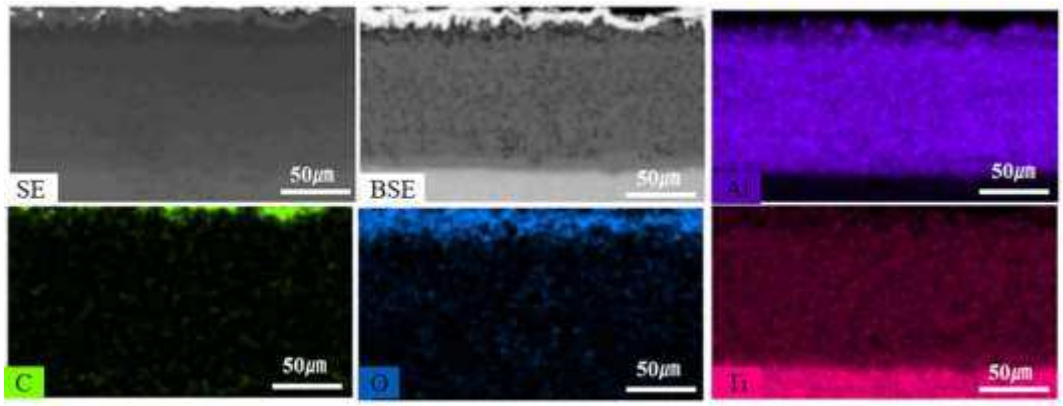

Figure 3. EDS element maps of composite coating obtained by hot dip aluminizing (760°C×10min) and carburizing (1050°C×4h)

3.1.2. Growth kinetics of $TiAl_3$ phase

After hot dip aluminizing, the coating formed on the surface of Ti65 sample is composed of $TiAl_3$ phase +L-(Ti,Al) and L-(Ti,Al) layer. The relationship between the thickness and time of $TiAl_3$ phase can be expressed by the empirical formula [27, 28]:

$$d=kt^n \quad (1)$$

where d is the thickness of $TiAl_3$ phase (μm), t is the hot dip aluminization time (min), k is the rate constant, and n is the kinetic index. The kinetic index n <0.5 is diffusion controlled growth, and n > 0.5 is reaction controlled growth.

Preprints (www.preprints.org) | NOT PEER-REVIEWED | Posted: 23 June 2023 doi:10.20944/preprints202306.1678.v1

The thickness of $TiAl_3$ phase is represented by d_{TiAl_3}, and the growth kinetics curve of $TiAl_3$ phase was fitted by Equation (1), as shown in Figure 4:

$$d_{TiAl_3}=12.066t^{0.755} \quad (2)$$

The results show that the growth of $TiAl_3$ phase is reaction controlled growth.

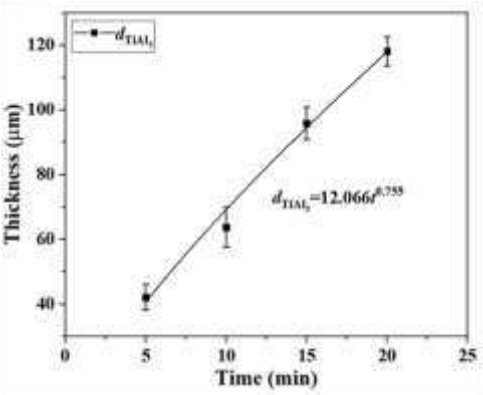

Figure 4. Growth kinetics curve of $TiAl_3$ phase

3.1.3 Growth kinetics of Ti-Al alloy phase layer

The d_5, d_{10}, d_{15}, and d_{20} are used to represent the thickness of Ti-Al alloy phase layer in the process of carburizing after 5min, 10min, 15min and 20min of hot dip aluminizing, respectively. The growth kinetics curve of Ti-Al alloy phase layer was fitted by Formula (1), as shown in Figure 5:

$$d_5=35.725t^{0.443} \quad (3)$$

$$d_{10}=56.503t^{0.441} \quad (4)$$

$$d_{15}=76.160t^{0.358} \quad (5)$$

$$d_{20}=114.050t^{0.487} \quad (6)$$

The results show that the growth of Ti-Al alloy phase layer is controlled by diffusion.

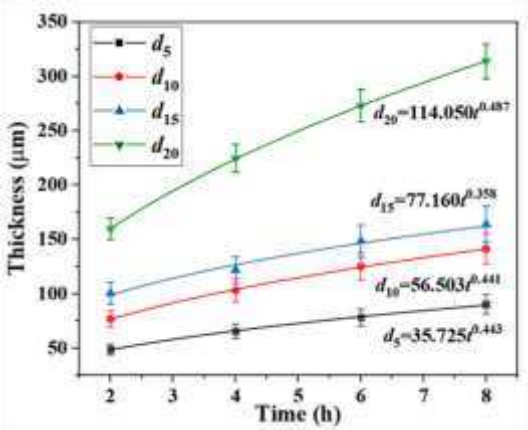

Figure 5. Growth kinetics curves of Ti-Al alloy phase layers in the process of carburizing under different hot dipping aluminizing times

3.1.4 Formation mechanism of composite coating

During hot dip aluminizing of titanium alloy, the liquid aluminum and the base metal interdiffuse and $TiAl_3$ phase is formed on the titanium alloy. The diffusion reaction is:

Preprints (www.preprints.org) | NOT PEER-REVIEWED | Posted: 23 June 2023 doi:10.20944/preprints202306.1678.v1

$$Ti+3Al \rightarrow TiAl_3 \quad (7)$$

Since the titanium atoms in the substrate diffuse into the liquid aluminum, which containes titanium atoms, and there are voids in the $TiAl_3$ phase, the liquid aluminum containing titanium atoms will partially fill the voids around $TiAl_3$ during hot dip aluminizing, forming a mixed phase layer of $TiAl_3$ phase and L-(Ti,Al) phase. When the titanium alloy sample is extracted from the aluminum pool, the liquid aluminum containing titanium atoms will adhere to the outside of the mixed phase layer and solidify into the outermost layer of the hot dip aluminized coating. So the coating after hot dip aluminizing is composed of $TiAl_3$ phase +L-(Ti,Al) mixed phase layer and L-(Ti,Al) layer.

When the hot dip aluminized Ti65 sample is carburized, the aluminum element in $TiAl_3$ phase continues to diffuse to the substrate, while the Ti element in the substrate diffuses to the coating. During the diffusion process, Al and Ti react to form three Ti-Al alloy layers (Ti_3Al, TiAl and $TiAl_2$). Kattner et al calculated the Gibbs free energy of the three products as follows:

$$\Delta Gf\ (TiAl_2) = -43858.4 + 11.02077T(K) \quad (8)$$

$$\Delta Gf\ (TiAl) = -37445.1 + 16.79376T(K) \quad (9)$$

$$\Delta Gf\ (Ti_3Al) = -29633.6 + 6.70801T(K) \quad (10)$$

At 1050°C, the Gibbs free energy of the three phases is less than zero, namely, $\Delta Gf < 0$, indicating that the three compounds can be formed thermodynamically. The formation process of alloy phase layer is:

$$2TiAl_3 + 4Ti \rightarrow Ti_3Al + TiAl + 2TiAl_2 \quad (11)$$

The natural transition of the three newly formed phases (Ti_3Al, TiAl and $TiAl_2$) and $TiAl_3$ not only ensure the high temperature oxidation resistance of the composite coating, but also enhance the interface bonding between the coating and the substrate, and slow down the propagation of microcracks through the coating.

The surface L-(Ti,Al) layer reacts with active carbon atoms to form Ti-Al carburizing layer, and finally forms Ti-Al alloy phase layer/Ti-Al carburizing layer composite coating.

The residual small amount of O_2 in the corundum crucible will cause the incomplete combustion of C to produce CO, and the energizer $BaCO_3$ will also produce CO during the decomposition process. Because there is a certain carbon concentration gradient and oxygen concentration gradient between the surface layer and the inner layer of the coating, and the temperature is relatively high, and the thermal vibration of the atoms is relatively severe, CO, C and O_2 will continue to diffuse inward through the L-(Ti,Al) layer, and the following reactions will occur in the L-(Ti,Al) layer and at the interface between the $TiAl_3$ phase:

$$4Al + 3O_2 \rightarrow 2Al_2O_3 \quad (12)$$

$$Ti + C \rightarrow TiC \quad (13)$$

$$2TiAl_3 + 3CO \rightarrow Al_2O_3 + 2TiAl_2 + 3C \quad (14)$$

The newly generated C and the C diffused from the carburizing agent will be polarized at the crystal defects with disordered atomic arrangement such as the boundary, grain boundary and dislocation of the L-(Ti,Al) layer and $TiAl_3$ phase, thus further distorting the interface, dislocation and other defects. These distortion regions will become

Preprints (www.preprints.org) | NOT PEER-REVIEWED | Posted: 23 June 2023 doi:10.20944/preprints202306.1678.v1

the rapid diffusion channels of CO, C and O_2. The Al in the L-(Ti,Al) layer is further oxidized into a continuous dense Al_2O_3 layer distributed in the Ti-Al carburizing layer outside the $TiAl_3$ phase, and $TiAl_3$ is further consumed to produce Al_2O_3 and $TiAl_2$. Since Ti content in L-(Ti,Al) layer is small and dispersing in Al, TiC generated during carburizing process will be dispersing in Ti-Al carburizing layer.

In the process of carburizing, the energizer $BaCO_3$ will react with Al and Ti atoms in the L-(Ti,Al) layer to form $BaAl_2O_4$ and $BaTiO_3$ at the top layer of the sample. The reaction is:

$$2BaCO_3+Ti+2Al+O_2 \rightarrow BaAl_2O_4+BaTiO_3+C+CO \quad (15)$$

3.2. High temperature oxidation resistance of coating

3.2.1. Microstructure of composite coatings after thermal exposure test

The interfacial reaction of the composite coating in the thermal exposure test is studied by observing the cross section morphology, EDS pattern and XRD pattern of the hot dip aluminizing (760°C×10min) and carburizing (1050°C×4h) Ti65 samples after different thermal exposure time. Figure 6 shows the sectional morphology of the composite coating after thermal exposure to static air at 800°C for 2 days and 16 days. After the thermal exposure test, micro-cracks appears in the coating[29]. As can be seen from Figure 6(b), micro-cracks do not penetrate the entire coating, but mainly distributes in the $TiAl_3$ phase layer with the largest thickness. This is because the natural transition of the four Ti-Al alloy phase layers significantly improves the interface bonding between the coating and the substrate, and slows down the further propagation of microcracks through the coating.

By comparing Figure 6(d) with Figure 1(b), it can be found that the thickness of Ti_3Al, TiAl and $TiAl_2$ phases increases after the thermal exposure test, while the thickness of $TiAl_3$ phases decreases. The part of L-(Ti,Al) around $TiAl_3$ phase is oxidized into Al_2O_3 and distributed between $TiAl_3$ phase and L-(Ti,Al). The Al_2O_3 content of heat exposure for 2 days is small and distributed outside L-(Ti,Al) in a fine network, while the Al_2O_3 content of heat exposure for 16 days is massive and significantly more than that of residual heat exposure for 2 days. Due to the increase of Ti content, L-(Ti,Al) near $TiAl_2$ phase has enough Ti atomic weight to react with Al in $TiAl_2$ phase to form $TiAl_2$. Therefore, a mixed phase layer of $TiAl_2$ and Al_2O_3 appears in the upper part of $TiAl_2$ phase. After 16 days of thermal exposure, a relatively continuous and dense $TiAl_2$ and Al_2O_3 layer was formed above the $TiAl_3$ phase layer. These changes in thermal exposure tests can effectively prevent oxygen from entering the substrate.

Figure 7 shows the EDS element maps of the composite coating after 16 days of thermal exposure. The results show that the oxygen content from the coating surface to the substrate shows a decreasing trend and oxygen is mainly distributed in the Ti-Al carbon layer. Therefore, the composite coating can effectively prevent oxygen from entering the substrate and protect the substrate from oxidation for a long time at 800°C. Figure 8(a), Figure 8(b) and Figure 8(c) are XRD patterns before thermal exposure test, for 2 days and for 16 days, respectively. Figure 8(b) adds Ti_2AlC and Al_4C_3 compared with Figure 8(a). Figure 8(c) compared with Figure 8(b), the contents of $TiAl_3$, C and Ti_2AlC decreases, while Al_4C_3, TiC and $BaTiO_3$ disappear, and TiO_2 and $BaAlTi_5O_{14}$ appear.

Preprints (www.preprints.org) | NOT PEER-REVIEWED | Posted: 23 June 2023 doi:10.20944/preprints202306.1678.v1

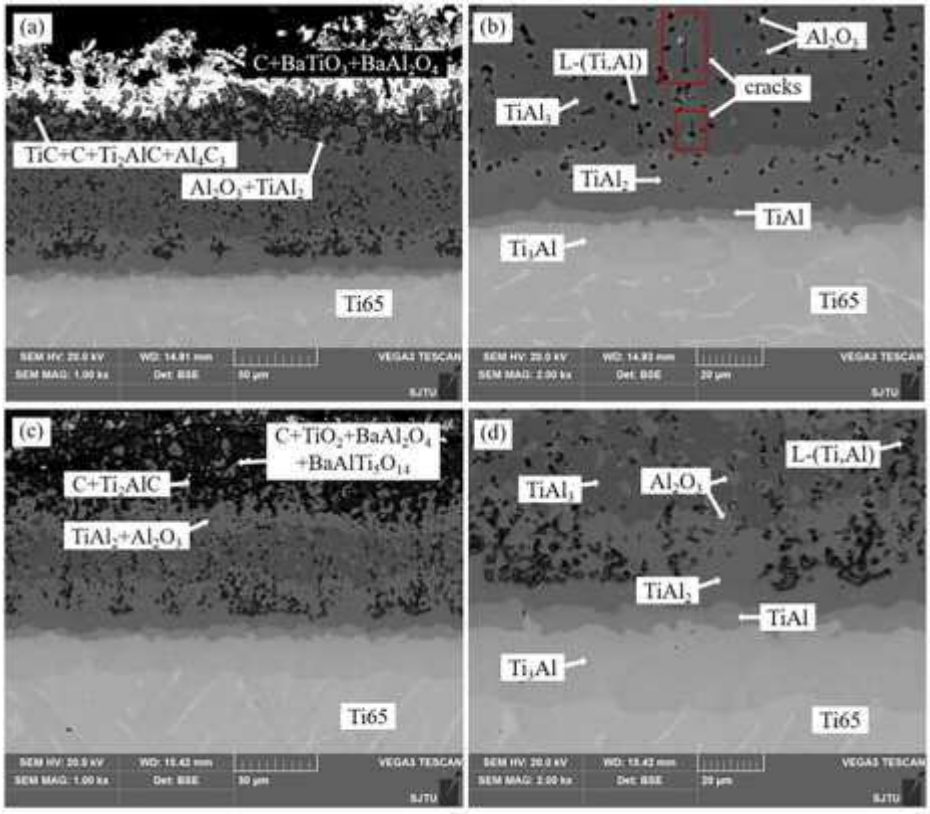

Figure 6. (a) Microstructure of the composite coating after thermal exposure for 2 days; **(b)** alloy phase morphology after thermal exposure for 2 days; **(c)** Microstructure of the composite coating after thermal exposure for 16 days; **(d)** alloy phase morphology after thermal exposure for 16 days

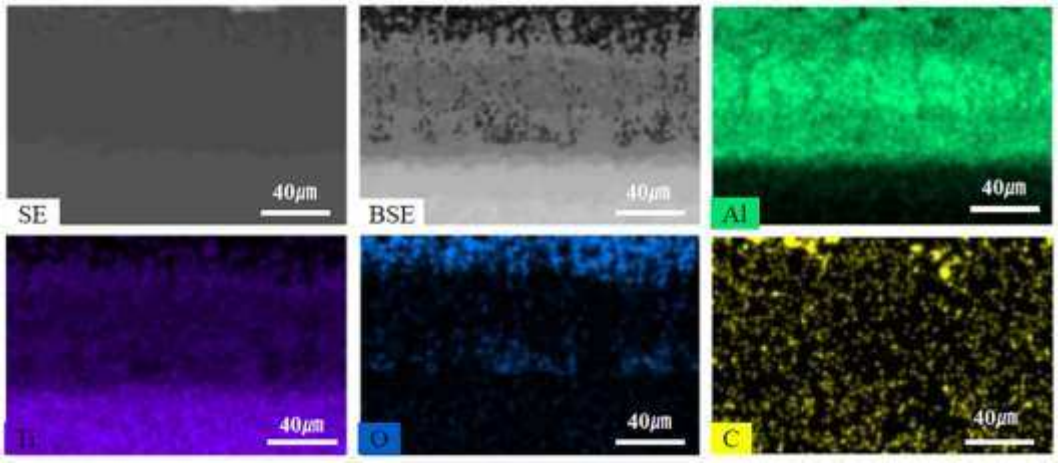

Figure 7. EDS element maps of composite coating after thermal exposure for 16 days in 800°C air

Preprints (www.preprints.org) | NOT PEER-REVIEWED | Posted: 23 June 2023 doi:10.20944/preprints202306.1678.v1

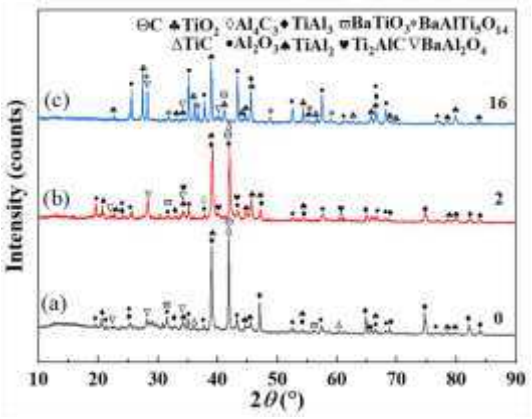

Figure 8. XRD pattern of composite coating: (a) before thermal exposure; (b) Heat exposure for 2 days; (c) Thermal exposure 16 days

3.2.2. High temperature oxidation weight gain curve

Figure 9 shows the oxidation kinetics curves of uncoated Ti65 sample, hot dip aluminization (760°C×10min) Ti65 sample, hot dip aluminization (760°C×10min) and carburizing (1050°C×4h) Ti65 sample (represented by groups A, B and C below) in the air at 800°C. The weight of all samples increases with the increase of thermal exposure time, and the weight of group A is significantly higher than that of group B and C.

The oxidation kinetics curve of group A samples can be fitted as follows:

$$\Delta m=14.702t^{0.7} \quad (16)$$

where, Δm is the oxidation weight gain (mg/cm^2) of group A samples, and t is the oxidation time (days).

The oxidation kinetics curve of group B samples can be fitted as follows:

$$\Delta m'=1.745t^{0.4} \quad (17)$$

where, $\Delta m'$ is the oxidation weight gain (mg/cm^2) of group B samples, and t is the oxidation time (days).

The oxidation kinetics curve of group C samples can be fitted as follows:

$$\Delta m''=1.010t^{0.25} \quad (18)$$

where, $\Delta m''$ is the oxidation weight gain (mg/cm^2) of group C samples, and t is the oxidation time (days).

The oxidation of group A samples, namely uncoated Ti65 substrate samples, is the most serious, indicating that the oxidation layer[5] (mainly TiO_2) of uncoated Ti65 substrate samples can not inhibit the further oxidation of the substrate at 800°C.After 16 days of thermal exposure, the weight gain of group A is 102.390 mg/cm^2, that of group B is 5.29mg/cm^2, and that of group C is 2.044mg/cm^2. The oxidation weight gain of group A is about 50 times that of group C, and the oxidation weight gain of group B is about 2.6 times that of group C, which means that the composite coating significantly improves the oxidation resistance of Ti65 alloy at high temperature.

In the process of thermal exposure test of group A samples, A large amount of oxide peel was shed[5], while in the whole process of thermal exposure test of group B samples, no oxide peel was shed and the surface of group B was kept smooth; in the process of thermal exposure test of group C samples, no obvious oxide peel was shed, but white

Preprints (www.preprints.org) | NOT PEER-REVIEWED | Posted: 23 June 2023 doi:10.20944/preprints202306.1678.v1

spot-like substances appeared on the coating surface. One of the reasons for the peeling of oxide skin is that the TiO_2 -rich oxide skin formed at 800°C has loose structure and weak adhesion with substrate. Another reason is the mismatch of thermal expansion coefficient between the oxide layer and the substrate.

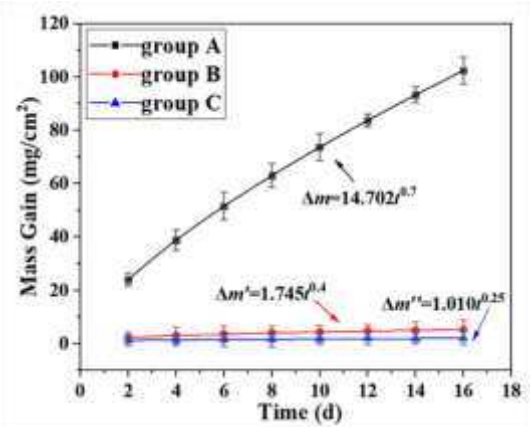

Figure 9. Oxidation kinetics curves of group A, B and C samples in 800°C air

3.2.3. Mechanism of oxidation resistance at high temperature

The process of thermal exposure is also a process of atomic diffusion. At high temperature, atomic diffusion intensifies and each element diffuses in the direction of decreasing concentration gradient. For example, Al, O and C elements diffuse to the inner layer and Ti elements diffuse to the outer layer. Ti_2AlC and Al_4C_3 appeared in the coating after 2 days of thermal exposure, indicating that the binding energy of Ti_2AlC and Al_4C_3 is large, which is not enough to form during the 4h carburizing process. Only when sufficient energy is obtained, it can form under the condition of high temperature and sufficient time. The formation process can be expressed as:

$$2Ti+Al+C \rightarrow Ti_2AlC \quad (19)$$

$$4Al+3C \rightarrow Al_4C_3 \quad (20)$$

With the increase of thermal exposure time, oxygen continues to diffuse inward. The oxygen reacts with the residual carbon in the depression of the coating surface to produce CO_2, and then reacts with the osmotic agent products $BaAl_2O_4$ and $BaTiO_3$. The Ti atom in the Ti-Al carburizing layer diffuses outwards and is oxidized by oxygen into TiO_2. TiO_2 and the oxidation products of $BaAl_2O_4$ and $BaTiO_3$ form the mixture $BaAlTi_5O_{14}$. The reaction at this interface is as follows:

$$C+O_2 \rightarrow CO_2 \quad (21)$$

$$Ti+O_2 \rightarrow TiO_2 \quad (22)$$

$$BaTiO_3+BaAl_2O_4+2Al+9TiO_2+3O_2 \rightarrow 2BaAlTi_5O_{14}+Al_2O_3 \quad (23)$$

Then oxygen will enter the Ti-Al carburizing layer, continue to react with the unoxidized Al in the carburizing process, and react with Ti atoms, TiC, Ti_2AlC and Al_4C_3.At the same time, TiC will react with Al and Ti. The reaction of the interface is as follows:

$$Ti+O_2 \rightarrow TiO_2 \quad (22)$$

$$4Al+3O_2 \rightarrow 2Al_2O_3 \quad (12)$$

Preprints (www.preprints.org) | NOT PEER-REVIEWED | Posted: 23 June 2023 doi:10.20944/preprints202306.1678.v1

$$TiC+2O_2 \rightarrow TiO_2+CO_2 \quad (24)$$

$$4Ti_2AlC+15O_2 \rightarrow 8TiO_2+4CO_2+2Al_2O_3 \quad (25)$$

$$Al_4C_3+6O_2 \rightarrow 2Al_2O_3+3CO_2 \quad (26)$$

$$TiC+Ti+Al \rightarrow Ti_2AlC \quad (27)$$

The structure of TiO_2 generated by oxidation in the Ti-Al carburizing layer is loose, and the escape of CO_2 will leave a void in the layer. The occurrence of these defects will destroy the continuity of the Al_2O_3 phase layer and promote the further inward diffusion of oxygen. After 16 days of thermal exposure, the contents of C and Ti_2AlC are reduced due to oxidation, TiC is oxidized to TiO_2 and converts to Ti_2AlC, and Al_4C_3 is completely oxidized and disappeared.

When oxygen passes through the Ti-Al carburizing layer to the $TiAl_3$ phase layer, it will react with $TiAl_3$, and the resulting oxidation products will form a relatively continuous and dense $TiAl_2$ and Al_2O_3 phase layer distributed on the interface between the $TiAl_3$ phase layer and Ti-Al carburizing layer. The reaction is as follows:

$$4TiAl_3+3O_2 \rightarrow 4TiAl_2+2Al_2O_3 \quad (28)$$

Oxygen penetrating into $TiAl_3$ phase layer will react preferentially with Al atoms in L-(Ti,Al) around $TiAl_3$ phase to generate Al_2O_3 distributed between $TiAl_3$ phase and L-(Ti,Al), namely:

$$4Al+3O_2 \rightarrow 2Al_2O_3 \quad (12)$$

Because the atomic weight of Ti in L-(Ti,Al) is too small to react, and L-(Ti,Al) near the $TiAl_2$ phase layer can react with the Al of L-(Ti,Al) to form $TiAl_2$ due to the complementary source of Ti atoms in the $TiAl_2$ phase:

$$Ti+2Al \rightarrow TiAl_2 \quad (29)$$

Therefore, a mixed phase layer of $TiAl_2$ and Al_2O_3 appears in the upper part of $TiAl_2$ phase.

During the thermal exposure test, the aluminum element in $TiAl_3$ phase continues to diffuse to the substrate, and Al and Ti continue to react, resulting in the increase of the thickness of $TiAl_2$, TiAl and Ti_3Al phase layers, while the thickness of $TiAl_3$ phase layer decreases due to consumption. The increase or decrease of each alloy phase layer thickness can be obtained by observing and comparing Figure 1(b) and Figure 6(d).

4. Conclusions

In this study, Ti-Al alloy phase layer/Ti-Al carburizing composite coating was formed on the surface of titanium alloy by the stepwise coating method of hot dipping aluminizing and then carburizing. The microstructure, formation mechanism and growth kinetics of the composite coating were systematically studied. At 800°C, The oxidation behavior of uncoated Ti65 sample, hot dip aluminization (760°C×10min) Ti65 sample, hot dip aluminization (760°C×10min) and carburizing (1050°C×4h) Ti65 sample during 2-16 days was observed and analyzed. The conclusion is as follows:

(1)During hot dip aluminizing of Ti65 sample, solid-liquid diffusion of Al and Ti atoms occurs on the surface of titanium alloy to form $TiAl_3$ phase +L-(Ti,Al) mixed phase layer and L-(Ti,Al) layer. After carburizing, the surface L-(Ti,Al) layer reacts with active carbon atoms to form Ti-Al carburizing layer. The aluminum element in the $TiAl_3$ phase

layer continues to diffuse to the substrate, and the titanium element in the substrate continues to diffuse to the coating. Al and Ti continue to react to form a series of Ti-Al alloy phase layers ($TiAl_2$, TiAl, Ti_3Al) from outside to inside. Finally, Ti-Al alloy phase layer/Ti-Al carburizing layer composite coating is formed.

(2)After 800°C×16 days of thermal exposure test, the oxidation kinetics curves of the three groups of samples all conform to the parabola law. In addition, the oxidation gain of uncoated Ti65 is about 50 times that of hot-dip aluminized and carburized Ti65, and the oxidation gain of hot-dip aluminized Ti65 is about 2.6 times that of hot-dip aluminized and carburized Ti65. Therefore, the composite coating has excellent oxidation resistance at high temperature.

(3)During the oxidation process, $TiAl_3$ is consumed by oxidation, but the loss of $TiAl_3$ has no obvious effect on the oxidation rate. This is because the mixed phase layer of $TiAl_2$ and Al_2O_3 formed during the oxidation process is relatively continuous and dense, and has good oxidation resistance at high temperature, which can effectively prevent the further diffusion of oxygen elements to the substrate. This indicates that the Ti65 samples coated with the composite coating have long-term stability in 800°C air (≥16 days).

Author Contributions: Investigation, Data curation, and Writing – original draft, W.Y.; Project administration, Methodology, and Writing – reviewed, F.L.. All authors have read and agreed to the published version of the manuscript.

Funding: This research was funded by the Science and Technology Project of Education Department of Hunan Province (No. 22A0100), Hunan Provincial Natural Science Foundation of China (No. 2021JJ30672), and "National Innovation and Entrepreneurship Training Program for College Students" project (No. 202210530036).

Institutional Review Board Statement: Not applicable.

Informed Consent Statement: Not applicable.

Data Availability Statement: Not applicable.

Acknowledgments: The authors gratefully acknowledge the support provided by Materials Intelligent Design College Students' Innovation and Entrepreneurship Education Center, Xiangtan University, Xiangtan, Hunan, China.

Conflicts of Interest: The authors declare no conflict of interest.

Reference

1. Dai, J.;Li, S.;Zhang, H.;Yu, H.;Chen, C.;Li, Y.Microstructure and high-temperature oxidation resistance of Ti-Al-Nb coatings on a Ti-6Al-4V alloy fabricated by laser surface alloying. *Surf. Coat. Technol.***2018**, *344*, 479-488. https://dx.doi.org/10.1016/j.surfcoat.2018.03.060.
2. Huang, L.;An, Q.;Geng, L.;Wang, S.;Jiang, S.;Cui, X.;Zhang, R.;Sun, F.;Jiao, Y.;Chen, X.;Wang, C.Multiscale Architecture and Superior High-Temperature Performance of Discontinuously Reinforced Titanium Matrix Composites. *Advanced Materials*.**2021**, *33*. https://dx.doi.org/10.1002/adma.202000688.
3. Li, B.;Zhou, H.;Liu, J.;Kang, C.Multiaxial fatigue damage and reliability assessment of aero-engine compressor blades made of TC4 titanium alloy. *Aerospace Science and Technology*.**2021**, *119*. https://dx.doi.org/10.1016/j.ast.2021.107107.

4. Zhang, X.;Chen, Y.;Hu, J.Recent advances in the development of aerospace materials. *Progress in Aerospace Sciences*.**2018**, *97*, 22-34. https://dx.doi.org/10.1016/j.paerosci.2018.01.001.
5. Dai, J.;Zhu, J.;Chen, C.;Weng, F.High temperature oxidation behavior and research status of modifications on improving high temperature oxidation resistance of titanium alloys and titanium aluminides: A review. *J. Alloy. Compd.*.**2016**, *685*, 784-798. https://dx.doi.org/10.1016/j.jallcom.2016.06.212.
6. Yuan, S.;Lin, N.;Zou, J.;Lin, X.;Liu, Z.;Yu, Y.;Wang, Z.;Zeng, Q.;Chen, W.;Tian, L.;Qin, L.;Xie, R.;Li, B.;Zhang, H.;Wang, Z.;Tang, B.;Wu, Y.In-situ fabrication of gradient titanium oxide ceramic coating on laser surface textured Ti6Al4V alloy with improved mechanical property and wear performance. *Vacuum*.**2020**, *176*. https://dx.doi.org/10.1016/j.vacuum.2020.109327.
7. Wang, D.Q.;Shi, Z.Y.;Teng, Y.L.Microstructure and oxidation of hot-dip aluminized titanium at high temperature. *Applied Surface Science*.**2005**, *250*, 238-246. https://dx.doi.org/10.1016/j.apsusc.2005.01.002.
8. Zhang, Z.G.;Peng, Y.P.;Mao, Y.L.;Pang, C.J.;Lu, L.Y.Effect of hot-dip aluminizing on the oxidation resistance of Ti-6Al-4V alloy at high temperatures. *Corrosion Science*.**2012**, *55*, 187-193. https://dx.doi.org/10.1016/j.corsci.2011.10.029.
9. Li, Z.W.;Gao, W.;Ying, D.Y.;Zhang, D.L.Improved oxidation resistance of Ti with a thermal sprayed Ti3Al(O)-Al2O3 composite coating. *Scripta Materialia*.**2003**, *48*, 1649-1653. https://dx.doi.org/10.1016/s1359-6462(03)00133-7.
10. Zhou, Z.;Xie, F.;Hu, J.A novel powder aluminizing technology assisted by direct current field at low temperatures. *Surf. Coat. Technol.*.**2008**, *203*, 23-27. https://dx.doi.org/10.1016/j.surfcoat.2008.07.021.
11. Chen, Y.;Newkirk, J.W.;Liou, F.Synthesizing Ti-Ni Alloy Composite Coating on Ti-6Al-4V Surface from Laser Surface Modification. *Metals*.**2023**, *13*. https://dx.doi.org/10.3390/met13020243.
12. Zhang, X.J.;Gao, Y.H.;Ren, B.Y.;Tsubaki, N.Improvement of high-temperature oxidation resistance of titanium-based alloy by sol-gel method. *Journal of Materials Science*.**2010**, *45*, 1622-1628. https://dx.doi.org/10.1007/s10853-009-4138-8.
13. Hu, X.;Li, F.;Shi, D.;Xie, Y.;Li, Z.;Yin, F.A design of self-generated Ti-Al-Si gradient coatings on Ti-6Al-4V alloy based on silicon concentration gradient. *J. Alloy. Compd.*.**2020**, *830*. https://dx.doi.org/10.1016/j.jallcom.2020.154670.
14. Wang, Z.;Li, F.;Hu, X.;He, W.;Liu, Z.;Tan, Y.Preparation of Ti-Al-Si Gradient Coating Based on Silicon Concentration Gradient and Added-Ce. *Coatings*.**2022**, *12*. https://dx.doi.org/10.3390/coatings12050683.
15. Wang, C.J.;Lee, J.W.;Twu, T.H.Corrosion behaviors of low carbon steel, SUS310 and Fe-Mn-Al alloy with hot-dipped aluminum coatings in NaCl-induced hot corrosion. *Surf. Coat. Technol.*.**2003**, *163*, 37-43. https://dx.doi.org/10.1016/s0257-8972(02)00588-1.
16. Han, S.;Li, H.;Wang, S.;Jiang, L.;Liu, X.Influence of silicon on hot-dip aluminizing process and subsequent oxidation for preparing hydrogen/tritium permeation barrier. *International Journal of Hydrogen Energy*.**2010**, *35*, 2689-2693. https://dx.doi.org/10.1016/j.ijhydene.2009.04.033.
17. Ren, X.;Wang, F.High-temperature oxidation and hot-corrosion behavior of a sputtered NiCrAlY coating with and without aluminizing. *Surf. Coat. Technol.*.**2006**, *201*, 30-37. https://dx.doi.org/10.1016/j.surfcoat.2005.10.042.
18. Khanna, R.;Kokubo, T.;Matsushita, T.;Nomura, Y.;Nose, N.;Oomori, Y.;Yoshida, T.;Wakita, K.;Takadama, H.Novel artificial hip joint: A layer of alumina on Ti-6Al-4V alloy formed by Micro-arc oxidation. *Materials Science & Engineering C-Materials for Biological Applications*.**2015**, *55*, 393-400. https://dx.doi.org/10.1016/j.msec.2015.05.021.
19. Parekh, T.;Patel, P.;Sasmal, C.S.;Jamnapara, N.I.Effect of plasma processed Ti-Al coating on oxidation and tensile behavior of Ti6Al4V alloy. *Surf. Coat. Technol.*.**2020**, *394*. https://dx.doi.org/10.1016/j.surfcoat.2020.125704.
20. Bai, H.;Zhong, L.;Kang, L.;Liu, J.;Zhuang, W.;Lv, Z.;Xu, Y.A review on wear-resistant coating with high hardness and high toughness on the surface of titanium alloy. *J. Alloy. Compd.*.**2021**, *882*. https://dx.doi.org/10.1016/j.jallcom.2021.160645.

21. Liu, J.-p.;Luo, L.-s.;Su, Y.-q.;Xu, Y.-j.;Li, X.-z.;Chen, R.-r.;Guo, J.-j.;Fu, H.-z.Numerical simulation of intermediate phase growth in Ti/Al alternate foils. *Transactions of Nonferrous Metals Society of China*.**2011**, *21*, 598-603. https://dx.doi.org/10.1016/s1003-6326(11)60756-5.
22. Goda, D.J.;Richards, N.L.;Caley, W.F.;Chaturvedi, M.C.The effect of processing variables on the structure and chemistry of Ti-aluminide based LMCS. *Mater. Sci. Eng. A-Struct. Mater. Prop. Microstruct. Process*.**2002**, *334*, 280-290. https://dx.doi.org/10.1016/s0921-5093(01)01894-9.
23. Martin, R.;Kampe, S.L.;Marte, J.S.;Pete, T.P.Microstructure/processing relationships in reaction-synthesized titanium aluminide intermetallic matrix composites. *Metallurgical and Materials Transactions a-Physical Metallurgy and Materials Science*.**2002**, *33*, 2747-2753. https://dx.doi.org/10.1007/s11661-002-0397-6.
24. Fu, E.K.Y.;Rawlings, R.D.;McShane, H.B.Reaction synthesis of titanium aluminides. *Journal of Materials Science*.**2001**, *36*, 5537-5542. https://dx.doi.org/10.1023/a:1012540927009.
25. Kong, L.;Qi, J.;Lu, B.;Yang, R.;Cui, X.;Li, T.;Xiong, T.Oxidation resistance of TiAl3-Al composite coating on orthorhombic Ti2AlNb based alloy. *Surf. Coat. Technol*.**2010**, *204*, 2262-2267. https://dx.doi.org/10.1016/j.surfcoat.2009.12.023.
26. Zhao, Y.G.;Zhou, W.;Qin, Q.D.;Liang, Y.H.;Jiang, Q.C.Effect of pre-oxidation on the properties of aluminide coating layers formed on Ti alloys. *J. Alloy. Compd*.**2005**, *391*, 136-140. https://dx.doi.org/10.1016/j.jallcom.2004.07.073.
27. Marder, A.R.The metallurgy of zinc-coated steel. *Progress in Materials Science*.**2000**, *45*, 191-271. https://dx.doi.org/10.1016/s0079-6425(98)00006-1.
28. Yang, W.;Park, J.;Choi, K.;Chung, C.H.;Lee, J.;Zhu, J.;Zhang, F.;Park, J.S.Evaluation of growth kinetics of aluminide coating layers on Ti-6Al-4V alloys by pack cementation and the oxidation behaviours of the coated Ti-6Al-4V alloys. *International Journal of Refractory Metals & Hard Materials*.**2021**, *101*. https://dx.doi.org/10.1016/j.ijrmhm.2021.105642.
29. Zhang, K.;Wang, Q.M.;Sun, C.;Wang, F.H.Preparation and oxidation resistance of a crack-free Al diffusion coating on Ti22Al26Nb. *Corrosion Science*.**2007**, *49*, 3598-3609. https://dx.doi.org/10.1016/j.corsci.2007.03.025.